

ANTENNA-COUPLED SUPERCONDUCTING TUNNEL JUNCTIONS WITH SINGLE-ELECTRON TRANSISTOR READOUT FOR DETECTION OF SUB-MM RADIATION

Thomas R. Stevenson,¹ Wen-Ting Hsieh,^{1,4} Mary J. Li,¹ Daniel E. Prober,³ Kee W. Rhee,⁵ Robert J. Schoelkopf,³ Carl M. Stahle,¹ John Teufel,³ Edward J. Wollack²

¹NASA/GSFC, Detector Systems Branch, Code 553, Greenbelt, MD 20771

²NASA/GSFC, Infrared Astrophysics Branch, Code 685, Greenbelt, MD 20771

³Dept. of Applied Physics, Yale University, P.O. Box 208284, New Haven, CT 06520

⁴Raytheon ITSS, Lanham, MD 20703

⁵Naval Research Laboratory, Electronics Sciences & Technology, Washington DC 20375

ABSTRACT

Antenna-coupled superconducting tunnel junction detectors have the potential for photon-counting sensitivity at sub-mm wavelengths. The device consists of an antenna to couple radiation into a small superconducting volume and cause quasiparticle excitations, and a single-electron transistor to measure currents through tunnel contacts to the absorber volume. We describe optimization of device parameters, and recent results on fabrication techniques for producing devices with high yield for detector arrays. We also present modeling of expected saturation power levels, antenna coupling, and rf multiplexing schemes.

INTRODUCTION

To take advantage of low background photon rates, space-based submillimeter-wave interferometers will require advances in detector sensitivity and speed. Integration of photon-counting detectors with low power readout electronics to make large-format arrays is desired. The single quasiparticle photon counter (SQPC) is a superconducting direct detector proposed¹ to meet these requirements. We give an overview of SQPC operating principles, the current state of development of this device, and its potential advantages.

DETECTOR CONCEPT AND FABRICATION

The SQPC is an antenna-coupled superconducting tunnel junction (STJ) detector with integrated rf single-electron transistor (RF-SET) readout amplifier. (See Fig.1). STJs have been used for energy-resolving detection of single photons at visible to x-ray wavelengths.² In an STJ detector, a SIS tunnel junction is biased below its superconducting gap, and dark current and detector noise decrease exponentially as the temperature is lowered since most electrons are bound into Cooper pairs. Photon absorption breaks pairs in proportion to energy absorbed, and the released quasiparticles give a fast ($\approx 1 \mu\text{s}$) current pulse. Figure 1a shows how we adapt a STJ for detection of sub-mm photons. The absorber volume is scaled in proportion to photon energy to submicron dimensions. Coupling of radiation to the small absorber is provided by an antenna. A normal metal trap speeds diffusion of quasiparticles away from the junction after tunneling to prevent slowing of the response by backtunneling.³ Sensitive and fast readout of photocurrents through the small, high-impedance tunnel junction is provided by an integrated RF-SET (Fig. 1b). A standard readout circuit for a photoconductor is the transimpedance amplifier. An ideal amplifier for implementing this circuit for a SQPC is the RF-SET.⁴ A SET is a very high performance electrometer based on the Coulomb blockade effect⁵ with sub-femtofarad input capacitance. A RF-SET⁶ integrates a SET with a LC circuit resonant at $\approx 1 \text{ GHz}$ to match SET output impedance to a high electron mobility transistor (HEMT).

We use optical lithography to fabricate substrates with antennas, inductors and capacitors for the rf circuits, and device contacts. We use electron-beam lithography to make SETs and SQPCs in one process. Figure 2b shows that we use two detector junctions in parallel to form a dc superconducting quantum interference

Contact information for T. R. Stevenson: Email: thomass@pop500.gsfc.nasa.gov

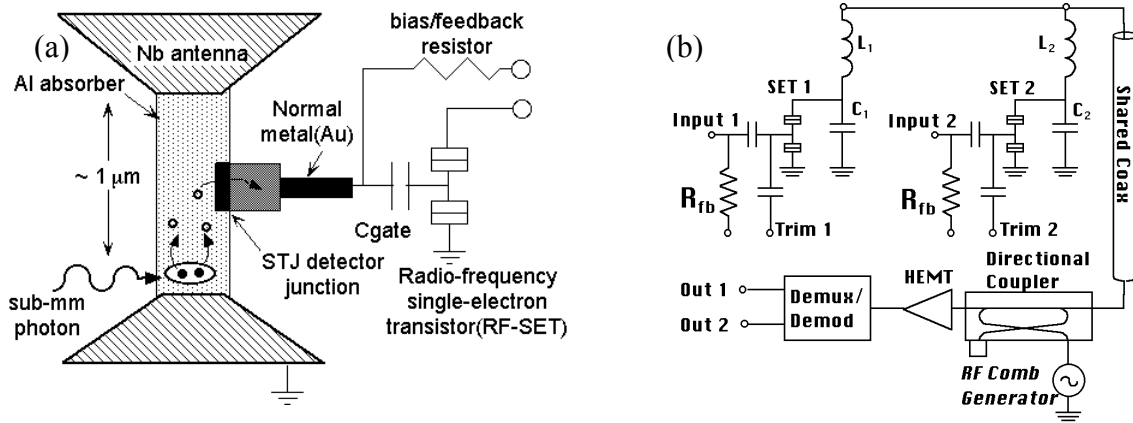


Figure 1: (a) SQPC: Absorption of radiation, coupled in by an niobium antenna, breaks Cooper pairs in an aluminum strip and gives a current pulse through a tunnel junction connected to a RF-SET. (b) RF-SET: an input gate signal changes both SET output impedance and amount of rf carrier power reflected by a resonant LC-circuit. Reflected power is amplified by a HEMT for detection at room temperature. Multiple RF-SETs with different resonant frequencies can share the same HEMT.

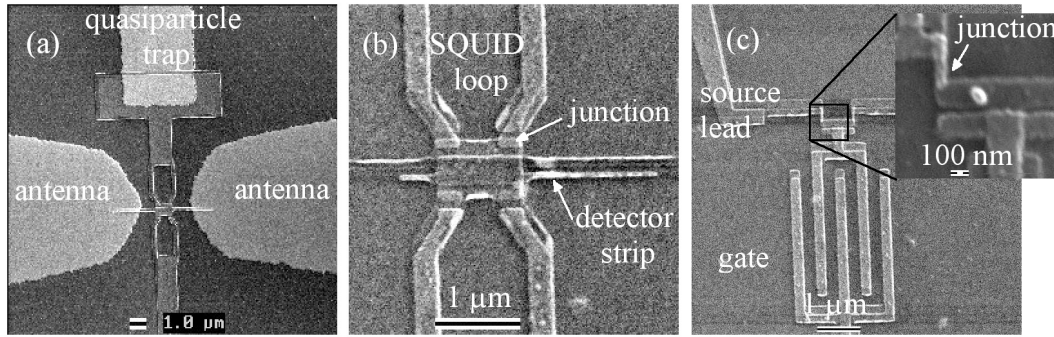


Figure 2: (a) SQPC detector strip and tunnel junctions are located between two halves of antenna; a gold quasiparticle trap is included here in wiring to just one of two dual detector SQUIDs. (b) Detector strip and tunnel junctions made by double-angle deposition of aluminum. Pairs of junctions form dc SQUIDs for suppression of critical current with a magnetic field. (c) SET with 0.5 fF input gate is formed in same process. Source and drain leads are connected to island via 60 nm x 60 nm junctions.

device (SQUID) so the total critical current can be suppressed with a magnetic field, which is essential for bias stability and for low dark currents. Figure 2c shows a SET. We use a standard SET fabrication process using a resist bilayer.⁷ We have refined this process to improve yield, with the goal of achieving reproducibility needed for large arrays, and are continuing to improve device uniformity and stability.

OPTIMIZATION OF DEVICE PARAMETERS & EXPERIMENTAL RESULTS

Apart from antenna coupling efficiency, the factors determining SQPC sensitivity are: (i) detector responsivity, (ii) dark current shot noise, (iii) RF-SET voltage noise, (iv) Johnson noise in the feedback resistor, and (v) detector impedance. We predict Noise Equivalent Power (NEP) $\approx 1 \times 10^{-19}$ W/ $\sqrt{\text{Hz}}$ could be obtained with existing prototypes based on demonstrated levels of performance measured for each factor.

The SQPC responsivity is ideally e/Δ , where Δ is the energy gap of the absorber and e is the electronic charge. For aluminum, $e/\Delta \approx 5000$ A/W. Efficient charge collection depends on making the tunneling time short by confining the quasiparticles to a small absorber volume, and on avoiding sources of recombination other than with thermally generated quasiparticles. Using dual SQUIDs as shown in Fig. 2b, we have used one SQUID to inject a quasiparticle current into the common absorber, and see a strong response in the subgap I - V of the second SQUID which seems to indicate good confinement and collection in our devices.

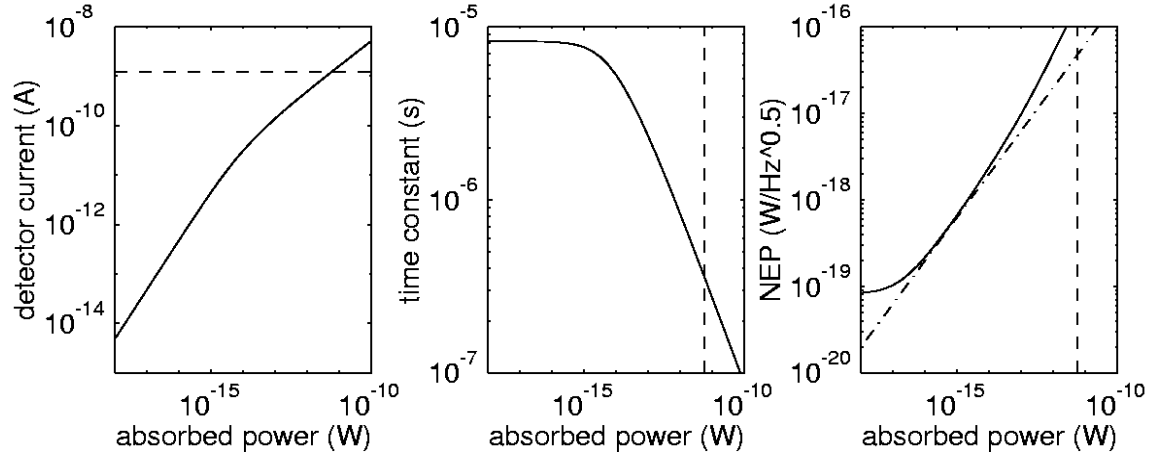


Figure 3: Simulated saturation effects for 300 GHz photons absorbed in an SQPC with 40 k Ω normal resistance, 0.023 (μm)³ absorber volume. Plots show power dependence of photocurrent, time constant, and NEP. Dash-dot line shows limiting NEP from photon shot noise. Dashed lines estimate current or power levels at which device will be driven normal.

We found detectors with ≈ 1 k Ω junctions deviated from BCS predictions for thermal dark current below ≈ 250 mK. The temperature-independent dark current was proportional to critical current squared, and was explainable as "rectification" of the Josephson oscillations occurring at a non-zero dc bias voltage.⁸ Since the minimum critical current of a dc SQUID is limited by self-inductance and junction asymmetry, we could not suppress the critical current to zero as is done for UV/optical or x-ray STJ detectors. Instead, we investigated junctions with smaller areas and higher resistance-area products. When the Josephson energy $E_J = I_c \Phi_0 / 2\pi$ was smaller than kT or the charging energy $E_c = e^2 / 2C_J$, we observed extra suppression of the critical current I_c by thermal or quantum fluctuations, and we measured BCS-like dark currents down to at least 250 mK with values of 2 pA or 0.5 pA for normal-state resistances of 10 k Ω or 40 k Ω respectively.

Nearly quantum-limited charge noise $\approx 10^{-6} e/\sqrt{\text{Hz}}$ has been demonstrated for RF-SETs with small input gates.⁹ However, it is difficult to maintain such sensitivity while providing strong coupling to an input signal. As gate coupling capacitance increases, the voltage noise, equal to the charge noise divided by gate capacitance, at first drops, but then levels off or increases as the charge noise of the RF-SET starts to degrade due to co-tunneling effects.⁴ We have obtained record SET voltage noise of 30 nV/ $\sqrt{\text{Hz}}$ with a 0.5 fF gate, and have been able to maintain noise close to this value during closed-loop operation.¹⁰

Table 1 summarizes the noise budget for a SQPC detector using demonstrated parameters. We assume our 0.5 pA device is used with a 100 M Ω integrated feedback resistor at 250 mK, with higher subgap impedance for the biased detector. The expected NEP is 1.2×10^{-19} W/ $\sqrt{\text{Hz}}$. Even better sensitivity is possible at lower temperature with a higher value feedback resistor.

Table 1: Detector sensitivity for demonstrated parameters

| Noise source | Parameters | Effective current noise |
|----------------------------|---------------------------|---|
| Dark current | 0.5 pA at 250 mK | 0.4 fA/ $\sqrt{\text{Hz}}$ |
| RF-SET voltage noise | 30 nV/ $\sqrt{\text{Hz}}$ | 0.3 |
| Johnson noise in R_{fb} | 100 M Ω at 250 mK | 0.4 |
| Total current noise | | 0.6 |
| NEP | | 1.2×10^{-19} W/$\sqrt{\text{Hz}}$ |

The maximum power level the SQPC can tolerate, and the expected background count rates in a space environment, will determine the maximum fractional bandwidth allowed for the incident radiation. As absorbed power increases, the concentration of quasiparticles in the absorber strip will grow, and the rate of self-recombination will increase. When self-recombination exceeds the tunneling rate, then the efficiency of charge collection drops. We have performed Monte Carlo simulations of the effects on signal and noise.

Preliminary results (Fig. 3) show that the saturation of the detector is quite gradual. With the expected background for space observations,¹¹ this model predicts background limited sensitivity for incident bandwidths of 0.1% to 100%. We consider weak saturation to be one advantage of the SQPC.

DESIGN OF ANTENNA COUPLING AND CALIBRATION

We have an experiment underway to measure the photoresponse of a SQPC to radiation. At this stage of development, we employ a simple bow-tie antenna. We estimate an antenna impedance¹² of $\sim 130\ \Omega$ and a SQPC sensor rf impedance of $20\sim 50\ \Omega$. This mismatch will be addressed in subsequent iterations. For an antenna on a silicon substrate, $\sim 97.5\%$ of the radiated power resides in the dielectric. We employ a quarter-wave-matching layer between dielectric and freespace to improve the coupling efficiency for radiation propagating through the dielectric. For initial measurements, a quasi-optically coupled "reverse bolometer" will be used as a thermal source in the sensor's field of view to produce a calculable radiometric flux. The physical temperature and emissivity as a function of frequency effectively control the source bandwidth.

MULTIPLEXING FOR ARRAYS

Multiplexing schemes will be crucial to the development of large-format arrays of any low-temperature detectors. RF-SETs have a natural wavelength division multiplexing capability⁴ (Fig. 1b). With a unique resonance frequency for each RF-SET, many RF-SETs can be individually or simultaneously powered and read out by a single HEMT following amplifier at 4 K. We have designed a 50-channel system with components based on measured parameters of lithographic rf circuits.¹³ For each pixel read out simultaneously, one wire is still required for the feedback resistor, and one for a weakly-coupled SET trim gate. Combining wavelength-division with some form of time-division, or other, multiplexing will be required to implement large arrays; however, the 50-fold reduction in output connections is quite valuable.

CONCLUSION

We have refined a fabrication process for SQPC detectors and RF-SET amplifiers with the goal of achieving the reproducibility needed for large-format arrays, and have recently attained large increases in device yield. With proper device design, we have attained subpicoamp dark currents, and record RF-SET voltage noise levels, which allow sensitivities of $1\times 10^{-19}\text{ W}/\sqrt{\text{Hz}}$ at temperatures as high as 250 mK. There is potential for even better sensitivity at lower temperatures, and the expected detector saturation behavior and multiplexing capability of RF-SETs enhance the potential for application of the SQPC in space-based submillimeter-wave interferometers.

ACKNOWLEDGMENTS

This work has been funded by GSFC Director's Discretionary Funds, NASA Explorer and Cross-Enterprise Programs, NASA Codes S & R, NASA NSG-8589.

REFERENCES

1. R. J. Schoelkopf, S. H. Moseley, C. M. Stahle, et al., IEEE Trans. Appl. Supercond. **9** 2935 (1999).
2. A. Peacock, P. Verhoeve, N. Rando, A. van Dordrecht, B. G. Taylor, et al., Nature **381** 135 (1996).
3. C. M. Wilson, L. Frunzio, K. Segall, L. Li, D. E. Prober, et al., Trans. Appl. Supercond. **11** 645 (2001).
4. T. R. Stevenson, A. Aassime, P. Delsing, et al., IEEE Trans. Appl. Supercond. **11** 692 (2001).
5. T. A. Fulton, G. J. Dolan, Phys. Rev. Lett. **59** 109 (1987).
6. R. J. Schoelkopf, P. Walgren, A. A. Kozhevnikov, P. Delsing, D. E. Prober, Science **280** 1238 (1998).
7. G. J. Dolan, Appl. Phys. Lett. **31** 337 (1977).
8. T. Holst, D. Esteve, C. Urbina, M. H. Devoret, 1994, Physica B **203**, 397.
9. A. Aassime, D. Gunnarsson, K. Bladh, P. Delsing, R. Schoelkopf, Appl. Phys. Lett. **79** 4031 (2001).
10. K. Segall, K. W. Lehnert, T. R. Stevenson, R. J. Schoelkopf, 2002, in preparation.
11. J. C. Mather, S. H. Moseley, D. Leisawitz, et al., astro-ph/9812454 (1998).
12. D. B. Rutledge, M. S. Muha, IEEE Trans. Antennas Propag., **AP-30** 535 (1982).
13. T. R. Stevenson, F. Pellerano, C. Stahle, K. Aidala, R. Schoelkopf, Appl. Phys. Lett. **80** (2002).